Asian Journal of Chemistry; Vol. 29, No. 10 (2017), 2299-2304

ASIAN JOURNAL OF CHEMISTRY

https://doi.org/10.14233/ajchem.2017.20791

Corrosion Behaviour of Some Phenyl Thiazole by Multiple Linear Regression Technique

R. SHANTHI* and R. JOEL KARUNAKARAN

Department of Chemistry, Madras Christian College, Tambaram, Chennai-600 045, India

*Corresponding author: E-mail: shanthi.ramani81@gmail.com

Received: 19 May 2017; *Accepted*: 15 July 2017; *Published online*: 31 August 2017; AJC-18538

Density functional theory methods B3LYP/6-31G(d,p) and PBE0/6-31G(d,p) were utilized and *ab inito* calculations were performed in RHF/3-21G(d,p) levels on the inhibitive effect of corrosion of four phenyl thiazole compounds namely amino phenylthiazole (APT), cinnamalidine aminophenylthiazole (CAPT), 2-salicylidine aminophenylthiazole (SAPT) and 2-vanilidine-amino-4-phenylthiazole (VAPT) on mild steel surface. The order of inhibition efficiency was found to be CAPT > VAPT > SAPT > APT. Most of the quantum chemical parameters used show agreement with this trend and the experimental and the calculated inhibition efficiency showed a good correlation.

Keywords: Corrosion, Multiple linear regression, Phenyl thiazoles, Corrosion behaviour.

INTRODUCTION

Metals and alloys are commonly used for the construction of underground transmission pipelines and flow lines. Acids are common chemicals used for multipurpose in chemical processes like descaling, acidifying and pickling [1-3]. Inhibition of corrosion is mostly carried out by compounds with carbonyl and amino functional groups are popular in the commercial world. Investigations have also been made on sulphur containing compounds like mercapto-5-triazole [4] and thiadiazole [5], benzotriazoles [6,7] and aminothiazoles [8].

The proper understanding of the behaviour of the inhibitor molecule on the surface of the metal helps in studying the corrosion behaviour of the molecule. The inhibitor molecule is either physically or chemically adsorbed on the surface of the corroding metal. It acts as a barrier on the surface preventing corrosion of the surface. The properties responsible for prevention of corrosion is attributed to the factors like size of the molecule, electron density of the donor atom, steric effect of the bulky group,orbital character of the donor atom and can be discussed in terms of their structure activity relationship. In addition to the above factors mentioned, the presence of π electrons in triple bond and double bond, aromatic ring also influence the corrosion behavior [9,10].

It has been proven that rather than individual carbonyl and amine functionalities, anils, the condensation products obtained from carbonyl and amino compound have more inhibition efficiency against acid corrosion [11]. The experimental inhibition of corrosion is taken from the previous experiment conducted [12]. The molecular structures of the investigated molecule is presented in Fig. 1. Possibilities of existence of an equilibrium between protonated and non-protonated species made us to investigate the protonated inhibitor species also.

COMPUTATIONAL METHODS

The optimization of molecular structure of the investigated inhibitors and their protonated form were done using Firefly software [13] which is partially based on GAMESS(US) [14]. In the present work the inhibition efficiency of the amino phenyl thiazole (APT) and its three anils are investigated through DFT method (B3LYP/6-31G(d,p)) [15-19] and PBE0/6-31G(d,p)) [20], *ab initio* method (RHF/3-21G(d,p)) [21-23]. The structure was visualized using Jmol software [24]. The molecular orbital composition analysis was done by using Multiwfn software [25]. The quantum chemical parameters were related to the inhibition efficiency using the following parameters.

E_{HOMO} and E_{LUMO}: Koopmans theorem [26] for closed shell of molecules is helpful to relate the quantum chemical parameters to the ionization potential (I) and the electron affinity (A). The energy of HOMO of the molecule is related inversely to the ionization potential of the molecule (eqn. 1). The ionization potential in turn is related to the donating ability of the molecule. A molecule with higher HOMO value has higher ability to donate electrons. In other words, a molecule behaves as a good inhibitor.

Energy of LUMO of a molecule is related to the electron affinity of the molecule (eqn. 1). The molecule with lower value of LUMO energy has more inhibition efficiency.

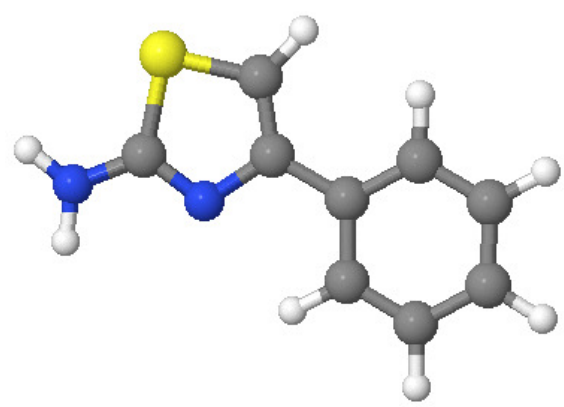

1: Amino phenylthiazole (APT)

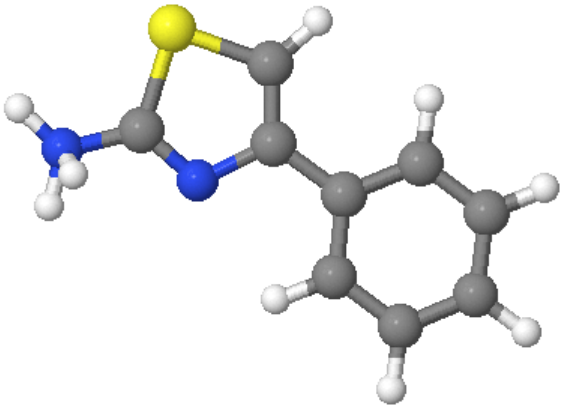

1a Cationic APT

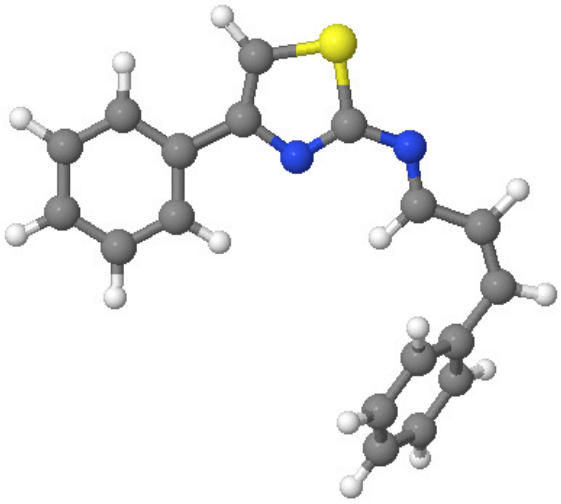

2: Cinnamalidene amino phenylthiazole (CAPT)

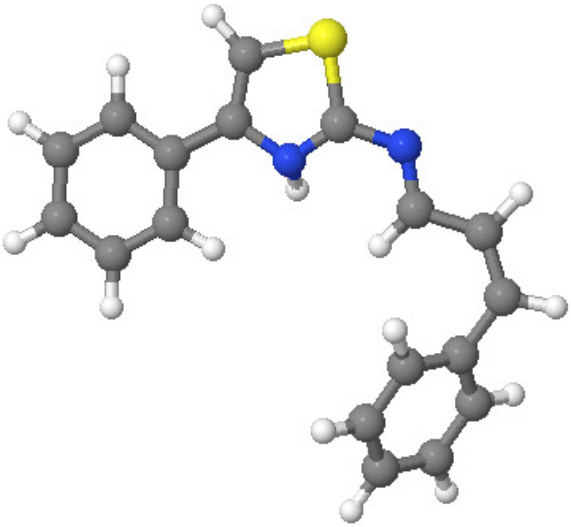

2a Cationic CAPT

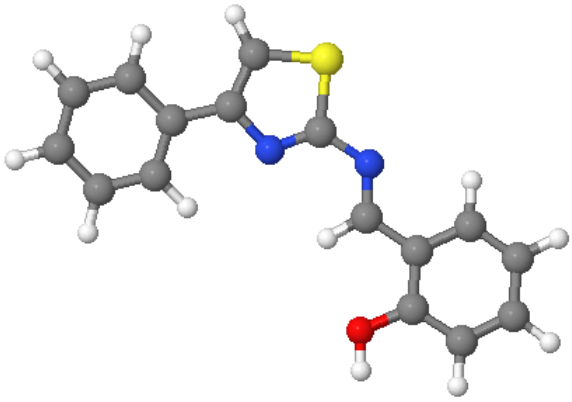

3: 2-Salicylidene amino phenylthiazole (SAPT)

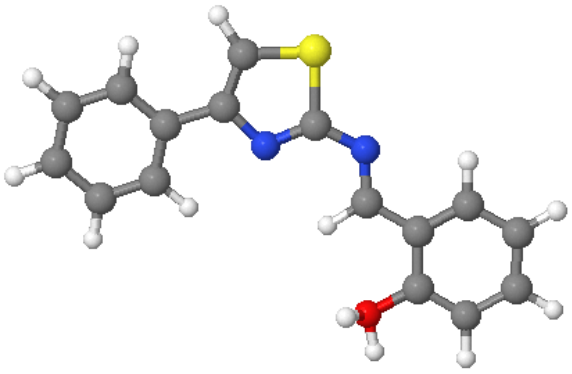

3a Cationic SAPT

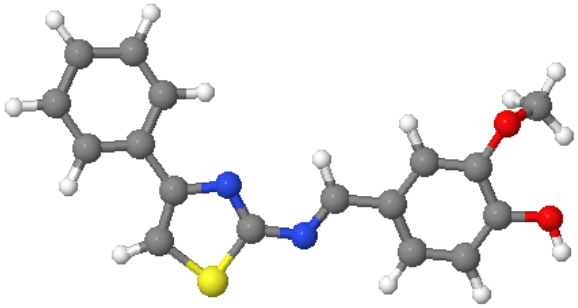

4: 2-Vanilidine amino phenylthiazole (VAPT)

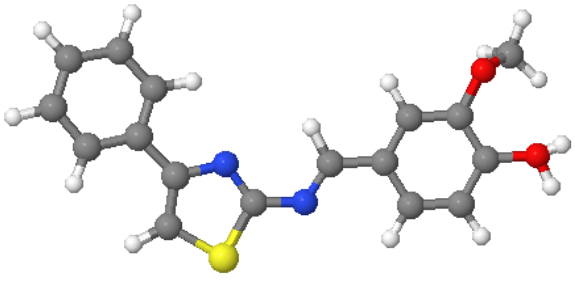

4a Cationic VAPT

Fig. 1. Structures of non-protonated and protonated inhibitor molecules

$$I = -E_{HOMO}, \quad A = -E_{LUMO} \tag{1}$$

Separation energy (ΔE): The major factor that is taken into account in predicting the quantum chemical behaviour of the molecule is the separation energy (ΔE). The best inhibitor molecule of the given series is characterized by it lower energy gap. The separation energy can be given by the difference between the E_{LUMO} and E_{HOMO}.

Electronegativity (X) and absolute hardness (η): The electronegativity and absolute hardness of the molecule is calculated with the energy of HOMO and LUMO (eqn. 2) [27,28]. The electronegativity of a molecule is related to its inhibition using Sanderson's electronegativity equalization principle [29]. The molecule with higher electronegativity is having a poor inhibition efficiency.

$$\text{Electronegativity } (\chi) = \frac{I + A}{2} \text{ and } \eta = \frac{I - A}{2} \tag{2}$$

Iczkowski and Margrave [30] proposed that the negative value of absolute hardness of the molecule is called as the chemical potential (μ). The inverse of the absolute hardness is called as the softness (σ) [31,32]. The higher value of softness indicates the higher inhibition efficiency [33].

Electrophilic index (ω) and dipole moment (D): The electrophilicity index can be given by the formula given by eqn. 3. Young and Parr [34] proposed that the electrophilicity index is the measure of lowering of energy due to maximum flow of electron from a donor system to an acceptor system. In a donor acceptor system, the value of electrophilicity index decides whether a molecule acts as a donor or acceptor.

$$\omega = \frac{\mu^2}{2\eta} \tag{3}$$

The number of electrons transferred can be calculated using eqn. 4. The computational values of $\chi_{Fe} = 7.0$ eV and $\eta_{Fe} = 0$ [35-37].

$$\Delta N = \frac{\chi_{Fe} - \chi_{inh}}{2(\eta_{Fe} + \eta_{inh})} \tag{4}$$

The variation of energy with the applied electric field is given by the dipole moment of the molecule, which measures the polarity of a polar covalent bond. It is defined as the product of charge on the atoms and the bond length between atoms (eqn. 5). The dipole moment is obtained from non-uniform distribution of charges on the various atoms in the molecule. The energy of the deformability, volume of the inhibitor molecules is directly proportional to dipole moment. This increases the contact area between the molecule and surface of metal and increasing the corrosion inhibition ability of inhibitors. The dipole moment of the inhibitor molecule cannot be related to the inhibition efficiency significantly [38-40].

$$D = q \times r \tag{5}$$

where q is the charge of the atom and r is the bond length between two atoms.

A good correlation have been observed between the corrosion behaviour of the organic compounds to the quantum chemical parameters like the frontier molecular orbital energy (E_{HOMO} and E_{LUMO}), electrophilicity index (ω), the absolute electronegativity (η) values, the fraction of electrons (ΔN) transfer from inhibitors to metals [41-43].

RESULTS AND DISCUSSION

The quantum chemical of the inhibition of corrosion was analyzed for the series of molecule in both protonated and non-protonated forms. The experimental trend was reported to be CAPT > VAPT > SAPT > APT [12].

The analysis of Table-1 shows that the CAPT molecule has the lowest energy gap (ΔE) non-protonated form and hence higher inhibition efficiency.This is consistent with the experimental results. The inhibitors can be arranged on the basis of energy gap, in non-protonated form as CAPT < VAPT < SAPT < APT. Lower energy gap indicates higher reactivity of the inhibitor molecule and hence its inhibition efficiency. The energy of LUMO of the CAPT molecule is also found to be less. The energy of LUMO indicates the tendency of the molecule to accept electrons. If this serves the decisive factor for inhibition of corrosion, the non-protonated form follows the experimental trend observed while the protonated form doesn't show such a trend.

The calculated electronegativities of the inhibitor molecules shows the trend CAPT > VAPT > SAPT > APT in non-protonated consistent with experimental results (Table-2).

The calculated hardness of the molecule predicts the back donating ability of the molecule. If the back donation occurs then the energy is proportional to the hardness of the molecule. This implies that for the given family of inhibitors, if the hard-

TABLE-1
CALCULATED ENERGIES OF HOMO AND LUMO AND THE ENERGY GAP
($\Delta E = E_{LUMO} - E_{HOMO}$) FOR INHIBITORS AND PROTONATED INHIBITORS (eV)

Method	1	2	3	4	1a	2a	3a	4a
				RHF/3-21G(d,p)				
E_{HOMO}	-7.758	-7.886	-7.850	-7.801	-11.570	-11.774	-9.894	-10.370
E_{LUMO}	2.988	1.586	1.668	1.709	-1.668	-2.803	-1.396	-2.141
ΔE	10.746	9.472	9.518	9.510	9.902	8.971	8.498	8.229
				B3LYP/6-31G(d,p)				
E_{HOMO}	-5.431	-5.722	-5.486	-5.513	-9.347	-9.328	-7.815	-8.229
E_{LUMO}	-0.7458	-2.237	-1.940	-1.995	-5.488	-6.299	-5.118	-5.671
ΔE	4.686	3.486	3.546	3.518	3.859	3.028	2.697	2.558
				PBE0/6-31G(d,p)				
E_{HOMO}	-5.673	-5.834	-5.733	-5.763	-9.622	-9.608	-8.068	-8.482
E_{LUMO}	-0.6095	-2.155	-1.828	-1.883	-5.331	-6.190	-5.018	-5.575
ΔE	5.064	3.679	3.905	3.880	4.291	3.418	3.050	2.907

TABLE-2
CALCULATED ELECTRONEGATIVITIES (χ) (eV) OF STUDIED INHIBITORS

	RHF/3-21G(d,p)	B3LYP/6-31G(d,p)	PBE0/6-31G(d,p)		RHF/3-21G(d,p)	B3LYP/6-31G(d,p)	PBE0/6-31G(d,p)
1	2.386	3.088	3.143	**1a**	4.952	7.420	7.478
2	3.151	3.981	3.995	**2a**	7.289	7.815	7.899
3	3.091	3.714	3.782	**3a**	4.250	6.468	6.544
4	3.048	3.755	3.823	**4a**	6.256	6.950	7.029

ness increases then the interaction between the metal surface and the inhibitor increases and this leads to increase in inhibition efficiency. The hardness of the given series of molecule doesn't show any trend as that of the experimental one (Table-3).

The calculated softness of the molecules shows a trend CAPT > VAPT > SAPT > APT. This matches with the experimental trend (Table-4). As the inhibitor molecule is protonated the softness increases. In this case, the experimental trend is not observed.

The electrophilicity index of the molecule shows a trend CAPT > VAPT > SAPT > APT at the B3LYP level (Table-5). This is an indication that CAPT molecule accepts more electron than the remaining inhibitors. The same trend is observed in the case of protonated inhibitors also.The number of electrons transferred also shows the trend CAPT > VAPT > SAPT > APT. No direct relationship could be established between the dipole moment of the inhibitor and its inhibition efficiency.

Mulliken population analysis has been widely used to probe the adsorption center for the inhibitors. If a heteroatom is more negatively charged then it is bound to the metal through the donor acceptor mechanism. The electrophiles tend to attack more negative hetero atom and in general it is found from the Table-6 that the nitrogen atom 6 has excessive negative charge than other heteroatoms of the system. The SAPT molecule has an additional O atom to get adsorbed on the surface of the molecule, hence has more inhibition efficiency than VAPT molecule.

Non-linear regression technique: Quantitative structure activity relationship (QSAR) studies have revealed that no simple or direct relationship can relate the inhibition efficiency to the quantum chemical parameter. The quantum mechanical approach may well be able to predict whether a molecular structure is better for corrosion inhibition purposes, when only molecular structure is the factor involved in inhibition and all other factors like nature of surface is also void. Combination

TABLE-3
CALCULATED HARDNESS η (eV) OF STUDIED INHIBITORS

	RHF/3-21G(d,p)	B3LYP/6-31G(d,p)	PBE0/6-31G(d,p)		RHF/3-21G(d,p)	B3LYP/6-31G(d,p)	PBE0/6-31G(d,p)
1	5.374	2.343	2.532	**1a**	6.618	1.929	2.147
2	4.737	1.744	1.839	**2a**	4.487	1.514	1.709
3	4.759	1.774	1.952	**3a**	5.673	1.348	1.525
4	4.756	1.761	1.940	**4a**	4.114	1.278	1.453

TABLE-4
CALCULATED SOFTNESS σ (au^{-1}) OF STUDIED INHIBITORS

	RHF/3-21G(d,p)	B3LYP/6-31G(d,p)	PBE0/6-31G(d,p)		RHF/3-21G(d,p)	B3LYP/6-31G(d,p)	PBE0/6-31G(d,p)
1	5.063	11.614	10.747	**1a**	4.112	14.104	12.674
2	5.743	15.601	14.793	**2a**	6.064	17.969	15.924
3	5.717	15.337	13.937	**3a**	4.796	20.182	17.841
4	5.721	15.456	14.025	**4a**	6.614	21.277	18.727

TABLE-5
CALCULATED VALUE OF ELECTROPHILICITY INDEX (ω), NUMBER OF ELECTRONS TRANSFERRED (ΔN) AND DIPOLE MOMENT (D) IN DEBYE OF THE STUDIED INHIBITORS

	ω	ΔN(e)	D		ω	ΔN(e)	D
			RHF/3-21G(d,p)				
1	0.530	0.4293	1.793	1a	1.853	0.1547	6.524
2	1.048	0.4063	2.284	2a	5.921	-0.0322	12.224
3	1.004	0.4107	1.984	3a	1.591	0.3235	34.681
4	0.977	0.4155	2.953	4a	4.756	0.0904	24.013
			B3LYP/6-31G(d,p)				
1	2.035	0.8348	1.839	1a	14.269	-0.1089	6.199
2	4.544	0.8655	1.723	2a	20.169	-0.2692	12.744
3	3.888	0.9262	2.848	3a	15.512	0.1973	32.761
4	4.005	0.921	3.008	4a	18.881	0.0196	23.556
			PBE0/6-31G(d,p)				
1	1.951	0.7616	1.888	1a	13.020	-0.1113	6.209
2	3.151	0.8170	2.100	2a	18.258	-0.2630	12.717
3	3.663	0.8243	2.842	3a	14.041	0.1495	32.872
4	3.766	0.8188	3.002	4a	16.999	-0.0099	23.676

TABLE-6
MULLIKEN POPULATION ANALYSIS OF HETERO ATOMS OF THE INHIBITORS

		RHF/3-21G(d,p)	B3LYP/6-31G(d,p)	PBE0/6-31G(d,p)			RHF/3-21G(d,p)	B3LYP/6-31G(d,p)	PBE0/6-31G(d,p)
	N1	-0.7550	-0.4991	-0.5110		N1	-0.6328	-0.4276	-0.4394
1	S5	0.3809	0.2047	0.2538	**1a**	S5	0.5579	0.3723	0.4214
	N6	-0.7230	-0.6186	-0.6551		N6	-0.5595	-0.5693	-0.6049
	N1	-0.7121	-0.5745	-0.5058		N1	-0.8223	-0.5235	-0.5561
2	S5	0.4679	0.4399	0.3154	**2a**	S5	0.6201	0.4220	0.4729
	N6	-0.7130	-0.5670	-0.4839		N6	-0.7539	-0.4388	-0.4515
	N1	-0.7142	-0.4926	-0.5067		N1	-0.7060	-0.4902	-0.5045
3	S5	0.4603	0.2528	0.3080	**3a**	S5	0.5307	0.3320	0.3852
	N6	-0.7485	-0.4859	-0.5022		N6	-0.6793	-0..4501	-0.4653
	O32	-0.6157	-0.5557	-0.5654		O32	-0.4965	-0.4574	-0.4668
	N1	-0.7145	-0.4934	-0.5070		N1	-0.7519	-0.4840	-0.4975
	S5	0.4643	0.2516	0.3066		S5	0.5017	0.3074	0.3606
4	N6	-0.7427	-0.4872	-0.5030	**4a**	N6	-0.7158	-0.4683	-0.4844
	O18	-0.7220	-0.5300	-0.5314		O18	-0.6067	-0.4602	-0.4641
	O32	-0.6026	-0.5477	-0.5559		O32	-0.6303	-0.6069	-0.6210

of more than one quantum chemical parameters are related to the average inhibition efficiency by using non-linear relationship was found to hold good [44,45].

Lukovits *et al.* [46] proposed a non-linear model (LKP) to study the interaction of the inhibitors with metal surfaces in acidic solution. This model utilized here is based on the Langmuir adsorption isotherm. Adsorption or coverage of the surface of the metal by the inhibitor is the major reason for inhibition of corrosion [47]. Bearing this concept, the surface of the metal covered is related as $\theta_i \approx E_i$.

According to linear model, the calculated inhibition efficiency is given by eqn. 6.

$$IE_{cal} = Ax_jC_j + B \quad (6)$$

where, IE_{cal} is the calculated efficiency of the inhibitor molecule, A and B are the regression co-efficient and x_j is a characteristic quantum index for the inhibitor and C_j denotes the concentration of inhibitor molecule. This approach was not satisfactory for correlating the results obtained in current experiments.

Hence, a non-linear multiple regression analysis was made using eqn. 7.

$$E_i = \frac{(Ax_j + B)C_i}{1 + (Ax_j + B)C_i} \quad (7)$$

The experimental inhibition efficiencies of the inhibitors are found in three different concentrations 1×10^{-3} M, 8×10^{-4} M, 6×10^{-4} M (500, 400 and 300 ppm, respectively) are found by potentiodynamic polarization method (Table-7) [12]. The experimental data is utilized here for all the four compounds. X_j is considered as the composite index of three quantum chemical parameter E_{HOMO}, E_{LUMO}, μ. Quantum chemical parameters obtained by B3LYP/6-31G (d,p) method is utilized for this purpose. A non-linear relationship is obtained as given by eqn. 8.

$$IE_i = \frac{(989.3 * E_{LUMO} - 868.52 * E_{HOMO} - 631.02 * D + 175.78)C_i}{1 + (989.3 * E_{LUMO} - 868.52 * E_{HOMO} - 631.02 * D + 175.78)C_i} \quad (8)$$

The coeffecient of determination (R^2) relates the percentage of variation in variable Y, which is explained by all the X variables together. The coeffecient of determination obtained between experimental efficiencies and the calculated efficiency is good and acceptable ($R^2 = 0.929$). The correlation coefficient (r) explains the degree of agreement between two variables namely experimental IE % and the calculated IE %. In the present case, the value of correlation coefficient is 0.963. This means the degree of agreement is 96 %, which is quite satisfactory.

Conclusion

The analysis of E_{LUMO}, electronegativity, softness, electrophilicity index and number of electrons transferred for the inhibitor in non-protonated form shows a complete agreement with experimental trend. The non-linear regression analysis also shows a good correlation coefficient.

REFERENCES

1. I. Ahamad and M.A. Quraishi, *Corros. Sci.*, **51**, 2006 (2009); https://doi.org/10.1016/j.corsci.2009.05.026.
2. Q.B. Zhang and Y.X. Hua, *Electrochim. Acta*, **54**, 1881 (2009); https://doi.org/10.1016/j.electacta.2008.10.025.
3. W. Li, Q. He, C. Pei and B. Hou, *Electrochim. Acta*, **52**, 6386 (2007); https://doi.org/10.1016/j.electacta.2007.04.077.
4. S.S. Mahmoud and E.G.A. Malidy, *Egypt. J. Chem.*, **39**, 365 (1996).
5. X.J. Raj and N. Rajendran, *Int. J. Electrochem. Sci.*, **6**, 348 (2011).

TABLE-7
EXPERIMENTAL AND CALCULATED INHIBITION EFFICIENCIES OF THE INHIBITOR MOLECULES

Inhibitor concentration (M)	1×10^{-3}		8×10^{-4}		6.6×10^{-4}	
	IE_{exp}	IE_{cal}	IE_{exp}	IE_{cal}	IE_{exp}	IE_{cal}
APT	80.0	74.9	68.6	70.5	62.5	66.4
CAPT	65.7	64.8	62.9	59.6	51.4	54.9
SAPT	54.3	55.0	51.4	49.5	48.6	44.7
VAPT	51.4	52.2	42.9	46.6	42.9	41.9

6. R.M. Souto, V. Fox, M.M. Laz, M. Pérez and R.S. González, *J. Electroanal. Chem.*, **411**, 161 (1996); https://doi.org/10.1016/0022-0728(96)04566-4.
7. G. Trabanelli, G. Brunoro, C. Monticells and M. Foganolo, Proceedings of the 9th ICMC, Toronto, Canada, June (1984).
8. D.D.N. Singh, M.M. Singh, R.S. Chaudhary and C.V. Agarwal, *J. Appl. Electrochem.*, **10**, 587 (1980); https://doi.org/10.1007/BF00615480.
9. F. Bentiss, M. Lebrini, H. Vezin and M. Lagrenée, *Mater. Chem. Phys.*, **87**, 18 (2004); https://doi.org/10.1016/j.matchemphys.2004.05.040.
10. S.T. Selvi, V. Raman and N. Rajendran, *J. Appl. Electrochem.*, **33**, 1175 (2003); https://doi.org/10.1023/B:JACH.0000003852.38068.3f.
11. M.N. Desai, M.B. Desai, C.B. Shah and S.M. Desai, *Corros. Sci.*, **26**, 827 (1986); https://doi.org/10.1016/0010-938X(86)90066-1.
12. M.A. Quraishi, M. Wajid Khan, M. Ajmal, S. Muralidharan and S. Venkatakrishna Iyer, *Anti-Corros. Methods Mater.*, **43**, 5 (1996); https://doi.org/10.1108/eb007386.
13. A. Alex, Granovsky, Firefly version 8.2.0, www.http://classic.chem.msu.su/gran/firefly/index.html.
14. M.W. Schmidt, K.K. Baldridge, J.A. Boatz, S.T. Elbert, M.S. Gordon, J.H. Jensen, S. Koseki, N. Matsunaga, K.A. Nguyen, S. Su, T.L. Windus, M. Dupuis and J.A. Montgomery, *J. Comput. Chem.*, **14**, 1347 (1993); https://doi.org/10.1002/jcc.540141112.
15. C. Lee, W. Yang and R.G. Parr, *Phys. Rev. B*, **37**, 785 (1988); https://doi.org/10.1103/PhysRevB.37.785.
16. A.D. Becke, *J. Chem. Phys.*, **98**, 5648 (1993); https://doi.org/10.1063/1.464913.
17. R. Ditchfield, W.J. Hehre and J.A. Pople, *J. Chem. Phys.*, **54**, 724 (1971); https://doi.org/10.1063/1.1674902.
18. M.M. Francl, W.J. Pietro, W.J. Hehre, J.S. Binkley, M.S. Gordon, D.J. DeFrees and J.A. Pople, *J. Chem. Phys.*, **77**, 3654 (1982); https://doi.org/10.1063/1.444267.
19. W.J. Hehre, R. Ditchfield and J.A. Pople, *J. Chem. Phys.*, **56**, 2257 (1972); https://doi.org/10.1063/1.1677527.
20. C. Adamo and V. Barone, *J. Chem. Phys.*, **110**, 6158 (1999); https://doi.org/10.1063/1.478522.
21. J.S. Binkley, J.A. Pople and W.J. Hehre, *J. Am. Chem. Soc.*, **102**, 939 (1980); https://doi.org/10.1021/ja00523a008.
22. K.D. Dobbs and W.J. Hehre, *J. Comput. Chem.*, **7**, 359 (1986); https://doi.org/10.1002/jcc.540070313.
23. K.D. Dobbs and W.J. Hehre, *J. Comput. Chem.*, **8**, 861 (1987); https://doi.org/10.1002/jcc.540080614.
24. Jmol: an open-source Java viewer for chemical structures in 3D. http://www.jmol.org/.
25. T. Lu and F. Chen, *J. Comput. Chem.*, **33**, 580 (2012); https://doi.org/10.1002/jcc.22885.
26. V.S. Sastri and J.R. Perumareddi, *Corrosion*, **53**, 617 (1997); https://doi.org/10.5006/1.3290294.
27. J.F. Janak, *Phys. Rev. B*, **18**, 7165 (1978); https://doi.org/10.1103/PhysRevB.18.7165.
28. R.G. Pearson, *Proc. Natl. Acad. Sci. USA*, **83**, 8440 (1986); https://doi.org/10.1073/pnas.83.22.8440.
29. R.T. Sanderson, *Science*, **121**, 207 (1955); https://doi.org/10.1126/science.121.3137.207.
30. R.P. Iczkowski and J.L. Margrave, *J. Am. Chem. Soc.*, **83**, 3547 (1961); https://doi.org/10.1021/ja01478a001.
31. V.S. Sastri and J.R. Perumareddi, *Corrosion*, **53**, 617 (1997); https://doi.org/10.5006/1.3290294.
32. D.-Q. Zhang, L.-W. Gao and G.D. Zhou, *Corros. Sci.*, **46**, 3031 (2004); https://doi.org/10.1016/j.corsci.2004.04.012.
33. I. Lukovits, E. Kalman and F. Zucchi, *Corrosion*, **57**, 3 (2001); https://doi.org/10.5006/1.3290328.
34. W. Yang and R.G. Parr, *Proc. Natl. Acad. Sci. USA*, **82**, 6723 (1985); https://doi.org/10.1073/pnas.82.20.6723.
35. P. Geerlings, F. De Proft and W. Langenaeker, *Chem. Rev.*, **103**, 1793 (2003); https://doi.org/10.1021/cr990029p.
36. G. Gao and C. Liang, *Electrochim. Acta*, **52**, 4554 (2007); https://doi.org/10.1016/j.electacta.2006.12.058.
37. G. Gece and S. Bilgic, *Corros. Sci.*, **52**, 3304 (2010); https://doi.org/10.1016/j.corsci.2010.06.005.
38. N. Khalil, *Electrochim. Acta*, **48**, 2635 (2003); https://doi.org/10.1016/S0013-4686(03)00307-4.
39. L.M. Rodríguez-Valdez, A. Martínez-Villafañe and D. Glossman-Mitnik, *J. Mol. Struct. THEOCHEM*, **713**, 65 (2005); https://doi.org/10.1016/j.theochem.2004.10.036.
40. A. Stoyanova, G. Petkova and S.D. Peyerimhoff, *Chem. Phys.*, **279**, 1 (2002); https://doi.org/10.1016/S0301-0104(02)00408-1.
41. T. Arslan, F. Kandemirli, E.E. Ebenso, I. Love and H. Alemu, *Corros. Sci.*, **51**, 35 (2009); https://doi.org/10.1016/j.corsci.2008.10.016.
42. B.D. Mert, M.E. Mert, G. Kardas and B. Yazici, *Corros. Sci.*, **53**, 4265 (2011); https://doi.org/10.1016/j.corsci.2011.08.038.
43. P. Udhayakala, T.V. Rajendiran and S. Gunasekaran, *J. Adv. Sci. Res.*, **3**, 71 (2012).
44. K.F. Khaled, K. Babic-Samardzija and N. Hackerman, *Electrochim. Acta*, **50**, 2515 (2005); https://doi.org/10.1016/j.electacta.2004.10.079.
45. H. Ashassi-Sorkhabi, B. Shaabani and D. Seifzadeh, *Appl. Surf. Sci.*, **239**, 154 (2005); https://doi.org/10.1016/j.apsusc.2004.05.143.
46. I. Lukovits, E. Kalman and G. Palinkas, *Corrosion*, **51**, 201 (1995); https://doi.org/10.5006/1.3294362.
47. I. Lukovits, K. Palfi, I. Bako and E. Kalman, *Corrosion*, **53**, 915 (1997); https://doi.org/10.5006/1.3290275.